Numerical simulation of film condensation on vertical plate embedded in metallic foams

Article · January 2011

DOI: 10.1504/PCFD.2011.04102

Numerical simulation of film condensation on vertical plate embedded in metallic foams

Y.P. Du, Z.G. Qu*, H.J. Xu, Z.Y. Li, C.Y. Zhao and W.Q. Tao

Key Laboratory of Thermal Fluid Science and Engineering of MOE,
Xi'an Jiaotong University,
Xi'an 710049, China
Fax: +86-29-82668036
E-mail: ypiondu@stu.xjtu.edu.cn
E-mail: zgqu@mail.xjtu.edu.cn
E-mail: hjxu.1015@stu.xjtu.edu.cn
E-mail: lizengy@mail.xjtu.edu.cn
E-mail: cyzhao@mail.xjtu.edu.cn
E-mail: wqtao@mail.xjtu.edu.cn
*Corresponding author

Abstract: Film condensation on vertical plate embedded in metal foams was numerically investigated based on some modification for Nusselt theory. Related numerical model was established by introducing Brinkman-Darcy model. Advection and inertial force in the condensate film were considered, from which the non-linear effect of cross-sectional temperature distribution on condensation heat transfer was also involved. Condensation characteristics were discussed and compared with those on smooth surface. Effects of key parameters on condensate film thickness were examined. Furthermore, with either the increase in porosity or the decrease in pore density, the condensate layer becomes thinner.

Keywords: film condensation; vertical plate; metal foams; film thickness.

Reference to this paper should be made as follows: Du, Y.P., Qu, Z.G., Xu, H.J., Li, Z.Y., Zhao, C.Y. and Tao, W.Q. (2011) 'Numerical simulation of film condensation on vertical plate embedded in metallic foams', *Progress in Computational Fluid Dynamics*, Vol. 11, Nos. 3/4, pp.261–268.

Biographical notes: Yanping Du is a PhD candidate in School of Energy and Power Engineering at Xi'an Jiaotong University. His current research is focused on the condensation heat transfer in metal foams.

Zhiguo Qu is now an Associate Professor in the School of Energy and Power Engineering at Xi'an Jiaotong University. He received his PhD in Power Engineering and Engineering Thermophysics from Xi'an Jiaotong University in 2005. His current research is mainly focused on the enhancement of heat transfer, phase change heat transfer.

Huijin Xu is a PhD candidate in the School of Energy and Power Engineering at Xi'an Jiaotong University. His research interest is concentrated in theoretical and numerical modelling on conjugate heat transfer in porous media.

Zengyao Li is now an Associate Professor in the School of Energy and Power Engineering at Xi'an Jiaotong University. His research theme is solar energy utilisation.

Changying Zhao is a Professor in the School of Energy and Power Engineering at Xi'an Jiaotong University. His research theme is heat transfer enhancement in porous media.

Wenquan Tao is now a Professor in the School of Energy and Power Engineering at Xi'an Jiaotong University. His current research is focused on numerical methods for transport phenomena in multi-scale systems.

This paper is a revised and expanded version of a paper entitled 'Numerical Simulation of Film Condensation in Metal Foam Filled Vertical Plate' presented at *Asian Symposium on Computational Heat Transfer and Fluid Flow*, Jeju, Korea, 20–23 October, 2009.

1 Introduction

Film condensation was investigated extensively (Nusselt, 1916; Dhir and Lienhard, 1971; Popiel and Boguslawski, 1978; Sukhatme et al., 1990; Cheng and Tao, 1994) for several decades due to its wide applicable scope for kinds of industrial cooling processes. Nusselt (1916) first analysed the thermal resistance and influence factors for film condensation phenomena of laminar flow on flat plate. It was concluded that heat conduction thermal resistance across the condensate film dominates the heat transfer process. Later, Dhir and Lienhard (1971) investigated film condensation on plane surface and horizontal circular tube while Popiel and Boguslawski (1978) studied the process on solid sphere, in which both of the surface heat transfer coefficients were obtained based on Nusselt theory. Film condensation on horizontal single tubes with enhanced surface for condensers was experimentally investigated by Sukhatme et al. (1990) and Cheng and Tao (1994). It was concluded that the deviation of experimental value and the analytical result with Nusselt theory is about 10%.

Film condensation on surfaces covered with porous medium was numerously involved (Jain and Bankoff, 1964; Liu et al., 1984; Cheng and Chui, 1984; Masoud et al., 2000; Kaviany, 1986; Wang et al., 2003, 2005, 2006; Char et al., 2001; Al-Nimer and AlKam, 1997; Chang, 2008; Ma and Wang, 1998). Jain and Bankoff (1964) analysed condensation of laminar flow on vertical wall embedded in a porous medium. The lateral mass flux for film condensation was obtained by Liu et al. (1984) using similarity method with the Darcy model for porous media. Transient film condensation was referred from Cheng and Chui (1984) and Masoud et al. (2000), while boundary layer analysis was conducted for film condensation in solid matrix by Kaviany (1986). Steady film condensation on a horizontal surface covered with porous medium was investigated by Wang et al. (2003, 2005, 2006). It was concluded that wavy surface can enhance the heat transfer rate in the condensate layer. Char et al. (2001) investigated the effect of heat conduction of wall on film condensation in the presence of porous medium. It was indicated that wall conduction reduced the local heat transfer coefficient and the dimensionless interfacial temperature compared with the isothermal plate. Al-Nimer and AlKam (1997) analytically studied condensation performance on vertical surfaces imbedded in a porous medium by neglecting the advection term in the energy equation and treating the temperature distribution perpendicular to the film flow direction as linear profile. Chang (2008) performed a semi-analytical study on the film condensation on a horizontal wavy plate embedded in a porous medium and found that the capillary force of porous structure can result in a two phase region above the plate. Ma and Wang (1998) numerically investigated film condensation on the porous layer–coated vertical surface, within which a porous region and an open region coexist. They also discussed the effect of porous layer on the film thickness and condensation heat transfer. Even though the previous works presented the performance of film condensation on smooth and porous surface, no work is done for condensation on metal-foam attached surfaces.

As a kind of special porous media, metal foams have attracted much research interests recently due to their excellent thermal, acoustic, mechanical and electro-magnetic properties. Especially, the successful implementation of various heat transfer devices with metal foams drives the investigation of heat transfer mechanisms in metal foams. Many achievements have been obtained for single phase and boiling heat transfer on metal foam surface, but few work has been published for condensation heat transfer in metal foams with unique topological morphology in which the phase change mechanism is different from general porous structures.

To this end, the present authors aim to explore condensation mechanisms on surfaces covered with metal foams and establish a numerical model for film condensation heat transfer within metal foams in which the non-linear temperature distribution in the condensation layer was solved. The non-linear temperature distribution in the condensate layer was discussed. The characteristics of condensation on the vertical plate embedded in metal foams were discussed and compared with those on smooth plate. The effects of Jacobi number, porosity and pore density on the film thickness were also examined in turn.

2 Numerical implementation

2.1 Problem description

Dry saturated vapour of water at atmospheric pressure is static near the vertical plate covered with metal foams. Due to the gravity, condensate fluid flows downward along the plate. The schematic diagram of the numerical domain is shown in Figure 1. The width W and length L of the computational domain are 5×10^{-4} m and 1 m, respectively. The flow direction of condensing water is denoted by x, whereas the thickness direction is denoted by y. The positive x direction is also the direction of gravity. The temperature of the plate is below the saturated temperature of the vapour so that condensation takes place favourably.

Figure 1 Computational domain and boundary conditions

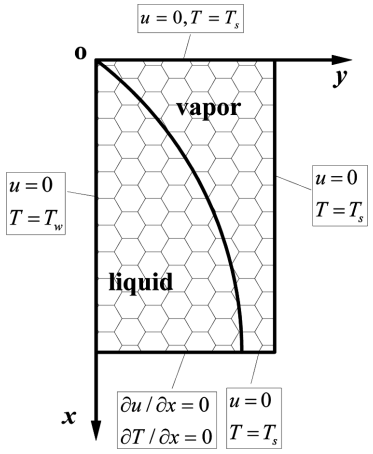

The effect of wall conduction and forced convection of the saturated gas are neglected due to the condition of unchanged temperature and zero velocity, respectively. Because of the complexity of the tortuosity of fluid flow in metal foams, laminar film condensation is supposed for simplification. The metal foams are assumed to be both isotropic and homogeneous. The fluid is considered to be incompressible with constant properties. Thermal radiation is ignored. Thermal dispersion effect is neglected as indicated in Calmidi and Mahajan (2000). The quadratic term for high-speed flow in porous medium are also neglected for momentum equation in the present study.

2.2 Governing equations and boundary conditions

Based on Nusselt theory, advection and inertial force in the condensate layer are all considered. Darcy model and local thermal equilibrium model are adopted for establishing the momentum equation and the energy equation. For condensate film of water, in the range of, $x \geq 0$, $0 \leq y \leq \delta(x)$, momentum equation is

$$\frac{\mu}{\varepsilon}\frac{\partial^2 u_l}{\partial y^2} - \frac{\mu}{K}u_l + g(\rho_l - \rho_v) = 0 \tag{1}$$

where K, g is the permeability of metal foams and acceleration of gravity, respectively. Correlation of permeability is referred from Lu et al. (2006) as follows:

$$K = 0.00073(1-\varepsilon)^{-0.224}(d_f/d_p)^{-1.11}d_p^2, \tag{2a}$$

$$d_f = d_p \cdot 1.18\sqrt{(1-\varepsilon)/(3\pi)}[1-\exp((\varepsilon-1)/0.04)]^{-1} \tag{2b}$$

$$d_p = 0.0254/\omega. \tag{2c}$$

where d_f and d_p are, respectively, fibre diameter and pore diameter and the variables u_l, ρ_l, ρ_v denote liquid velocity, liquid density and vapour density, respectively. Based on the liquid velocity distribution, the liquid mass flux at a certain location is shown as:

$$q_m = \int_0^{\delta(x)} \rho u_l \mathrm{d}y. \tag{3}$$

For the energy equation, the convective term is partially considered as velocity in the spanwise is consumed to be zero based on the Nusselt theory. Hence, the energy equation is expressed as:

$$u_l \frac{\partial T_l}{\partial x} = a_{el}\frac{\partial^2 T_l}{\partial y^2} \tag{4}$$

where, a_{el} means the effective thermal diffusivity in metal foams, whereas u_l and T_l is liquid velocity and temperature, respectively. In vertical wall for liquid film, the heat transferred through phase change of saturated vapour equals the heat conducted through the vertical wall along the thickness direction of the condensate layer to realise the heat balance.

$$r \cdot dq_m = k_l \cdot \left.\frac{\partial T_l}{\partial y}\right|_{y=0} \cdot \mathrm{d}x \tag{5}$$

where r, k_l, dq_m denote the latent heat of saturated water, liquid heat conductivity and the differential form of liquid film mass flux, respectively. For the convenience of numerical implementation, a square domain is selected as the computational domain. The boundary conditions of the governing equations in the whole computational domain for Equations (1) and (4) are shown in Figure 1. By iterative methods, the thickness of the condensate layer is obtained with Equations (1)–(5). The inner conditions at the liquid-vapour interface are set by considering the shear stress continuity as follows.

$$y = 0, \quad u = 0 \quad T = T_w \tag{6}$$

$$y = \delta(x), \quad \frac{\partial u_l}{\partial y} = 0 \quad T = T_s. \tag{7}$$

2.3 Numerical method

In the region outside the condensation layer of the computational domain, the domain extension method of Patankar (1980) is used. A very large value of the thermal conductivity and fluid viscosity are assigned to the fluid in this region to ensure the vapour static and saturated. At the boundary of the film layer, the $\partial u_l/\partial y = 0$ is assigned artificially to implement the boundary condition. Thus, the values in the extended domain cannot affect the solution of velocity and temperature field inside the condensation layer.

The governing equations in Equations (1) and (4) were solved with the SIMPLE algorithm (Tao, 2005). The convective terms are discritised with the power law scheme. A 200×20 grid system has been checked to gain a grid independent solution. The velocity field is solved ahead of the temperature field and the energy balance equation. By coupling of Equations (1)–(5), the non-linear temperature field in the condensation layer can be obtained. The thermal-physical properties in the numerical simulation, involving the fluid thermal conductivity, fluid viscosity, fluid specific heat, fluid density, fluid saturation temperature, fluid latent heat of vapourisation and gravity acceleration, are presented in Table 1.

Table 1 Constant parameters in numerical procedure

Parameter	ρ_l	ρ_v	μ_l	k_l	c_{pl}	T_s	r	g
Unit	kg/m^3	kg/m^3	Pa · s	W/(m · K)	J/(kg · K)	°C	J/kg	m/s^2
Value	977.8	0.58	2.825×10^{-4}	0.683	4200	100	297030	9.8

2.4 Validation

For a limit case of porosity being equal to 1, the present numerical model can predict the film condensation on vertical smooth plate for reference case validation. The distribution of film condensate thickness and local heat transfer coefficient on smooth plate predicted by the present

numerical model with those of Nusselt (1916), Al-Nimer and AlKam (1997) are shown in Figures 2 and 3 It can be seen that numerical solution is approximately consistent with either Nusselt (1916) or Al-Nimer and AlKam (1997) The maximum deviation for condensate thickness and local heat transfer coefficient is 14.5% and 12.1%, respectively, The reason for this deviation is due to that the non-linear effect of cross-sectional temperature distribution of liquid film is considered in the present model, whereas in the previous model, the linear distribution is only considered. Therefore, the feasibility of present numerical model is validated.

Figure 2 The distribution of condensate thickness for smooth plate (ε = 0.9, 10 PPI)

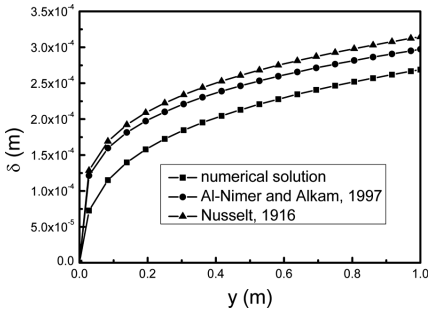

Figure 3 Local heat transfer coefficient for smooth plate (ε = 0.9, 10 PPI)

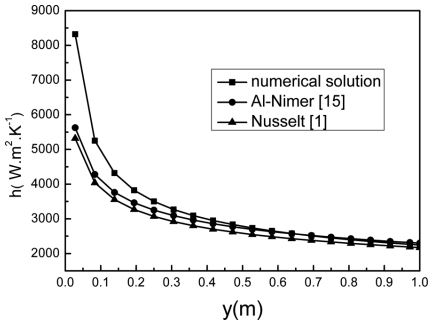

3 Parameter definitions

Some parameters used in this study are defined in this section. The Jacobi number is defined as follows:

$$\mathrm{Ja} = \frac{r}{c_{pl} \cdot (T_s - T_w)} \tag{8}$$

where T_s, T_w is saturated temperature and wall temperature. The effective thermal diffusivity in Equation (5) can be defined as Equation (6) shows.

$$a_{el} = \frac{k_e}{\rho_l \cdot c_{pl}} \tag{9}$$

where k_e is the effective thermal conductivity of metal foams and referred from paper (Boomsma and Poulikakos, 2001) as shown in the following:

$$k_e = \frac{1}{\sqrt{2}(R_A + R_B + R_C + R_D)} \tag{10}$$

$$R_{\mathrm{A}} = \frac{4\lambda}{(2e^2 + \pi\lambda(1-e))k_{\mathrm{s}} + (4 - 2e^2 - \pi\lambda(1-e))k_{\mathrm{l}}} \tag{11a}$$

$$R_{\mathrm{B}} = \frac{(e-2\lambda)^2}{(e-2\lambda)e^2 k_{\mathrm{s}} + (2e - 4\lambda - (e-2\lambda)e^2)k_{\mathrm{l}}} \tag{11b}$$

$$R_C = \frac{(\sqrt{2}-2e)^2}{2\pi\lambda^2(1-2\sqrt{2}e)k_s + 2(\sqrt{2} - 2e - \pi\lambda^2(1-2\sqrt{2}e))k_l} \tag{11c}$$

$$R_D = \frac{2e}{e^2 k_s + (4-e^2)k_l} \tag{11d}$$

$$\lambda = \sqrt{\frac{\sqrt{2}(2 - (5/8)e^3\sqrt{2} - 2\varepsilon)}{\pi(3 - 4\sqrt{2}e - e)}}, \quad e = 0.339 \tag{11e}$$

where k_{s} is the thermal conductivity of the solid and the value is adopted as $386\ \mathrm{W \cdot m^{-1} \cdot K^{-1}}$ in this paper. The local heat transfer coefficient and Nusselt number along the x direction can be obtained in Equations (12) and (13).

$$h(x) = \frac{k_e}{T_w - T_s}\frac{\partial T_l}{\partial y}\bigg|_{y=0} = \frac{1}{\delta(x)}\frac{k_e}{T_w - T_s}\frac{\partial T_l}{\partial [y/\delta(x)]}\bigg|_{y=0} \tag{12}$$

$$\mathrm{Nu}(x) = h(x)\frac{x}{k_e}. \tag{13}$$

The condensate film Reynolds number is expressed as

$$\mathrm{Re}(x) = \frac{4h(x)}{c_{pl} \cdot Ja \cdot \mu_l}. \tag{14}$$

4 Results and discussion

4.1 Temperature distribution in the condensate layer

Figure 4 exhibits the temperature distribution in condensate layer for three locations in the vertical direction (x/L = 0.25, 0.5 and 0.75) with porosity and pore density of being 0.9 and 10 PPI. It can be clearly seen that the temperature profile is nonlinear. The non-linear characteristic is more significant or the defined temperature gradient $\partial T_l/\partial[y/\delta(x)]$ is higher in the downstream of condensate layer than in the upper stream as the effect of heat conduction thermal resistance of the foam matrix in horizontal direction becomes more obvious in the downstream. Similar tendency can be found for the temperature distribution for various porosity and pore density at the same location of x/L = 0.5 as shown in Figures 5 and 6. It is found that the temperature is approaching linear distribution in the case of lower porosity and higher pore density for which the effective thermal conductivity is improved.

Figure 4 Temperature distribution in condensate layer for different x locations ($\varepsilon = 0.9$, 10 PPI)

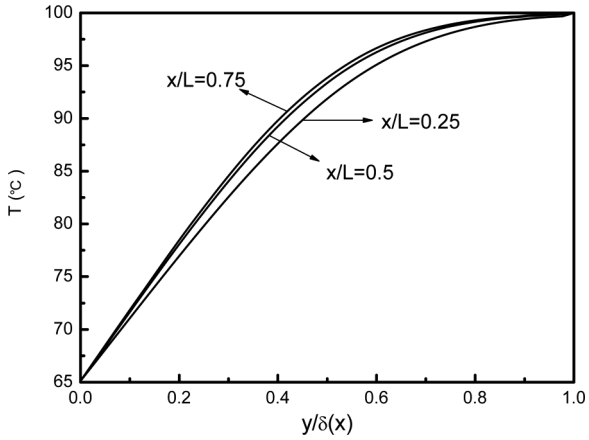

Figure 5 Temperature distribution in condensate layer for different porosities ($x/L = 0.5$, 10 PPI)

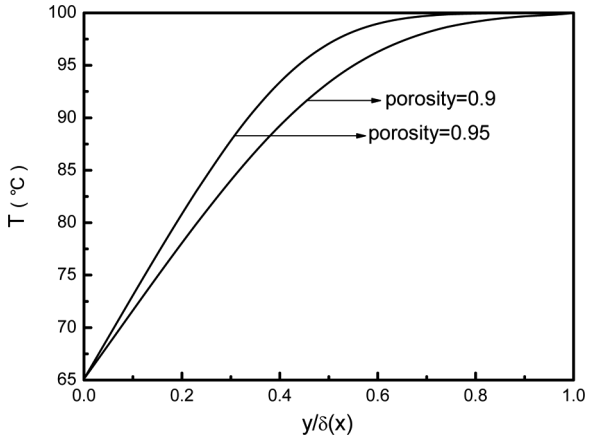

Figure 6 Temperature distribution in condensate layer for different pore densities ($x/L = 0.5$, $\varepsilon = 0.9$)

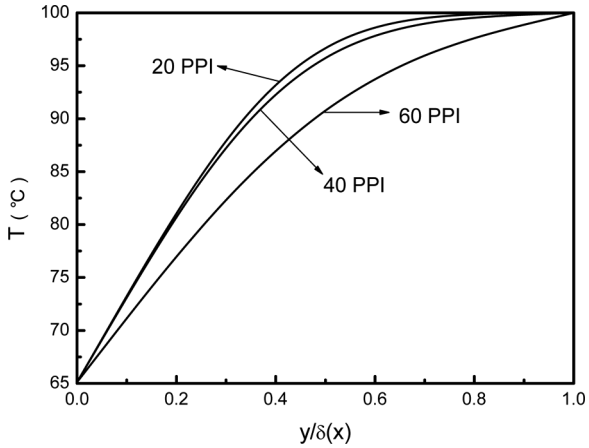

4.2 Comparison results with smooth plate

Condensation performance was compared with that on smooth plate to investigate the characteristic of condensation on metal foams covered plate. Distributions of condensation thickness, heat transfer coefficient and Nusselt number along the gravity direction are displayed in Figures 7–9. It can be seen that the film thickness of metal foams ($\varepsilon = 0.9$, 10 PPI) is larger than that of smooth plate for a fixed x position shown in Figure 7. This implies that metal foams thickened the condensate layer due to extra flow resistance caused by the foam matrix, which is negative for film condensation heat transfer. Although the defined wall temperature gradient $\partial T_l/\partial[y/\delta(x)]$ increases along the vertical direction, the film thickness also increases. Hence, the local heat transfer coefficient along the vertical plate is gradually decreased along the vertical direction as indicated in Equation (12). The final heat transfer coefficient distribution is shown in Figure 8. It is also found that the local heat transfer coefficient for foam surface is lower than smooth surface, but the difference between the heat transfer coefficient of the metal-foam surface and that of the smooth plate is approximately unchanged. This can be attributed to the two factors dominating the heat transfer process in metal-foam covered plate: the increased film thickness stated above and the improved effective thermal conductivity of foam matrix compared with smooth plate. The two factors compete in the whole heat transfer process. Finally, the former factor prevails in the whole process and later factor restricts the expanding trend of the two heat transfer coefficient difference in the downstream region of the condensate layer.

Figure 7 The distribution of thickness of condensate layer ($\varepsilon = 0.9$, 10 PPI)

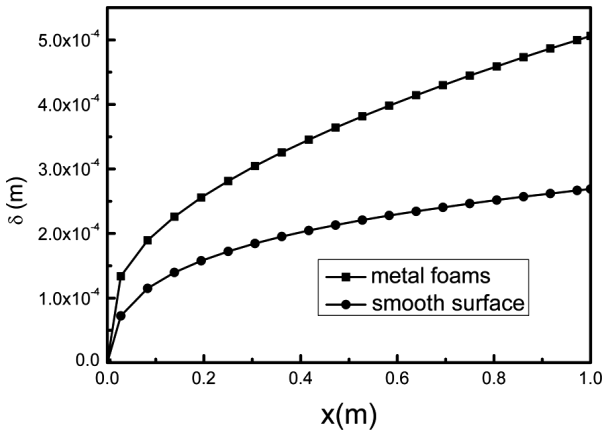

Figure 8 Heat transfer coefficient along gravity direction ($\varepsilon = 0.9$, 10 PPI)

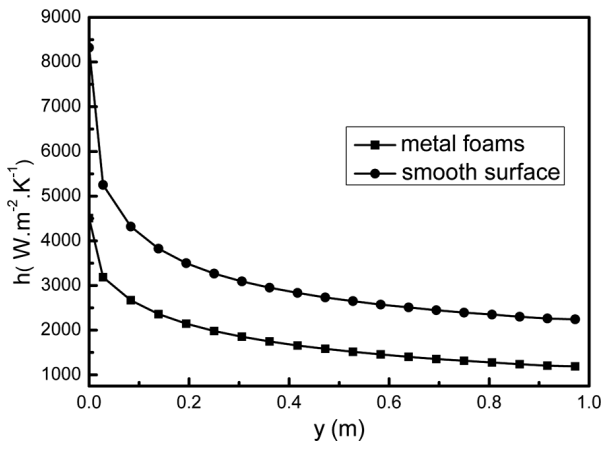

Figure 9 Nu as a function of condensate thickness ($\varepsilon = 0.9$, 10 PPI)

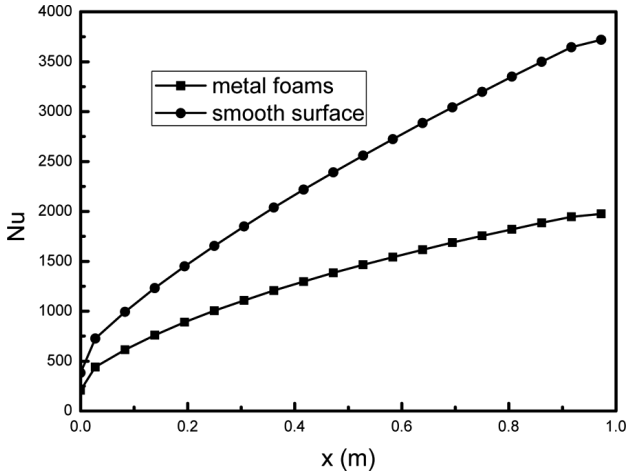

Figure 10 presents the local Nusselt number distribution defined in Equation (13) for the foam surface ($\varepsilon = 0.9$, 10 PPI) and smooth plate along the vertical direction. The characteristic length for the definition of Nu number is treated as x, which is not fixed and increases when the film thickness increases. Hence, the difference of Nu number between foam surface and smooth surface continuously increases along the vertical direction.

Figure 10 The distribution of Re along positive vertical direction ($\varepsilon = 0.9$, 10 PPI)

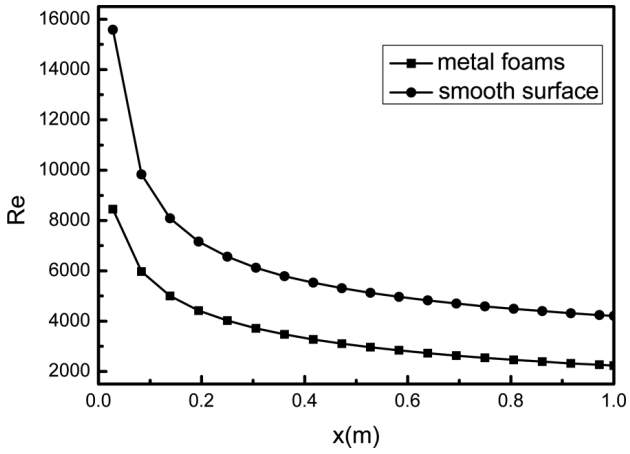

4.3 The characteristics of condensation on metal-foam covered surface

Figure 10 exhibited the distribution of Reynolds number defined in Equation (14) for condensation on the smooth plate and the metal foam-adhered surface ($\varepsilon = 0.9$, 10 PPI). It is obvious in Figure 10 that Reynolds number reduces and becomes flat along positive x direction, which is the same as the local heat transfer coefficient distribution. Moreover, it is smaller on metal foams covered surface than that on flat plate for the low permeability of metal foams. The characteristics of Nusselt number divided by Reynolds number vs. location is shown in Figure 11. It is found that the Nu/Re along vertical direction is linear to position and not relevant to the morphology of plate surface.

Figure 11 The distribution of Nu/Re ($\varepsilon = 0.9$, 10 PPI)

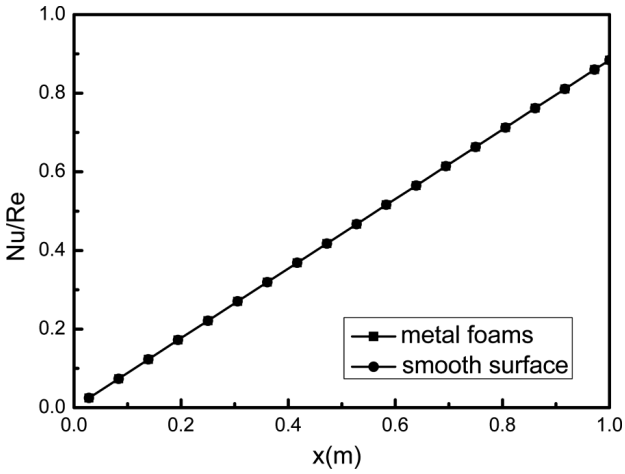

4.4 The effects of different factors on film condensation

The effects of parameters, involving Jacobi number, porosity and pore density, are discussed in this section. Super cooling degree can be controlled by changing the value of Ja. The effect of Ja on the condensate layer thickness is shown in Figure 12. It can be seen that condensate layer thickness decreases as Jacobi number increases. This can be attributed to the fact that the super cooling degree, which is the key factor to drive the condensation process, is reduced as Ja number increase to lead to a thinner liquid condensate layer. For a limit case of zero super cooling degree, the condensation cannot happens and the condensate layer does not exist. The effect of porosity on the condensate film thickness is shown in Figure 13. It is found that for a fixed position, the increase in porosity can lead to the decrease in the condensate film thickness, which is helpful for film condensation. This can be attributed to the fact that the increase in porosity can make the permeability of the metal foams increase and decreases the flow resistance of liquid flowing downwards. The effect of pore density on the condensate film thickness was shown in Figure 14. It can be seen that for a fixed x position, the increase in pore density can make the condensate film thickness increase greatly, which enlarges the thermal resistance of the condensation heat transfer process. The reason for the above result is that the increasing of pore density can greatly reduce the metal foam's permeability and then can substantially increase the flow resistance of the flowing-down condensate. Thus, with either the increase in porosity or the decrease in pore density, the condensate layer thickness is reduced for condensation heat transfer coefficient.

Figure 12 The effect of Jacobi number on the condensate thickness distribution (ε = 0.9, 10 PPI)

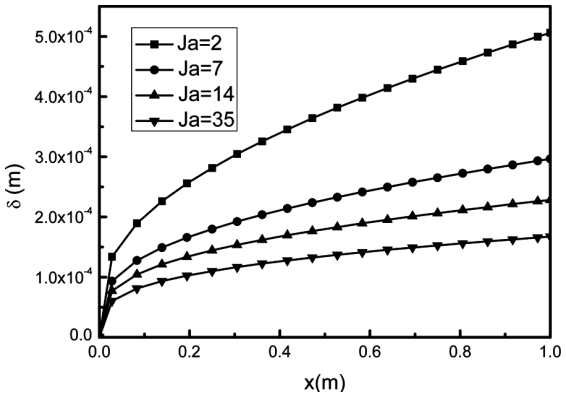

Figure 13 The effect of porosity on condensate thickness distribution (10 PPI)

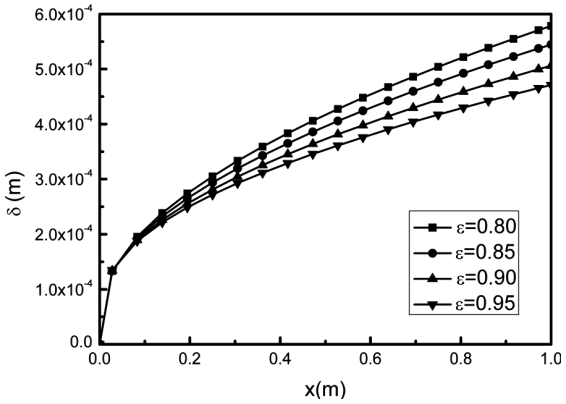

Figure 14 The effect of pore density on condensate thickness distribution (ε = 0.9)

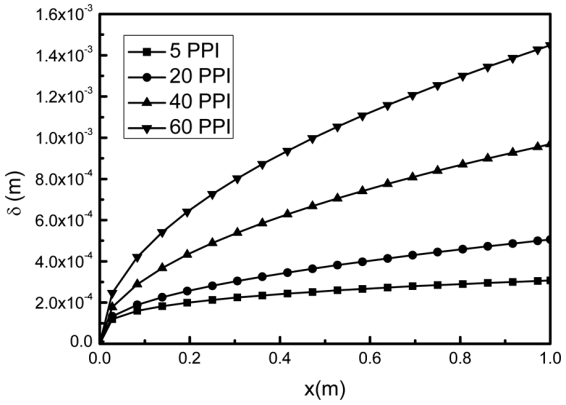

5 Conclusions

Numerical simulation of film condensation on vertical plate embedded in metal foams with one equation model was investigated by considering the advection term and inertial force in the condensate layer. The non-linear temperature distribution in the condensate layer is more significant in the downstream along the vertical direction due to the existence of foam matrix. The existence of metal foams reduces the thickness of condensate layer as well as the local heat transfer coefficient. The difference between the heat transfer coefficient of the metal foam-adhered plate and that of the smooth plate is approximately unchanged along positive gravity direction due to combined interaction of liquid permeability and effective thermal conductivity of the foam matrix. The parameter Nu/Re along vertical direction is linear to position and not relevant to the structure of foam or smooth surface. The film thickness can be thinned toward low permeability direction by either increase in porosity or decrease in pore density.

Acknowledgements

This work was supported by the National Natural Science Foundation of China (No. 50806057, 50876083), the National Key Projects of Fundamental R/D of China (973 Project: 2011CB610306), National Excellent Doctoral Dissertation Foundation of China (210141), Doctoral Fund of Ministry of Education of China (200806981013), and Program of New Century Excellent Talents in University (NCET-10-0640).

References

Al-Nimer, M.A. and AlKam, M.K. (1997) 'Film condensation on a vertical plate imbedded in a porous medium', *Applied Energy*, Vol. 56, pp.47–57.

Boomsma, K. and Poulikakos, D. (2001) 'On the effective thermal conductivity of a three- dimensionally structured fluid-saturated metal foam', *Int. J. Heat Mass Transfer*, Vol. 44, No. 4, pp.827–836.

Calmidi, V.V. and Mahajan, R.L. (2000) 'Forced convection in high porosity metal foams', *J. Heat Transfer*, Vol. 122, No. 3, pp.557–565.

Chang, T.B. (2008) 'Laminar film condensation on a horizontal wavy plate embedded in a porous medium', *International Journal of Thermal Sciences*, Vol. 47, pp.35–42.

Char, M.I., Lin, J.D. and Chen, H.T. (2001) 'Conjugate mixed convection laminar non-Darcy film condensation along a vertical plate in a porous medium', *International Journal of Engineering Science*, Vol. 39, pp.897–912.

Cheng, P. and Chui, D.K. (1984) 'Transient film condensation on a vertical surface in a porous medium', *Int. J. Heat Mass Transfer*, Vol. 27, pp.795–798.

Cheng, B. and Tao, W.Q. (1994) 'Experimental study on R-152a film condensation on single horizontal smooth tube and enhanced tubes', *ASME J. Heat Transfer*, Vol. 116, pp.266–270.

Dhir, V.K. and Lienhard, J.H. (1971) 'Laminar film condensation on plane and axisymmetric bodies in nonuniform gravity', *ASME J. Heat Transfer*, Vol. 93, pp.97–100.

Jain, K.C. and Bankoff, S.G. (1964) 'Laminar film condensation on a porous vertical with uniform suction velocity', *Trans. ASME, J. Heat Transfer*, Vol. 86, pp.481–489.

Kaviany, M. (1986) 'Boundary layer treatment of film condensation in the presence of a solid matrix', *Int. J. Heat Mass Transfer*, Vol. 29, pp.951–954.

Liu, C.Y., Ismail, K.A.R. and Ebinuma, C.D. (1984) 'Film condensation with lateral mass flux about a body of arbitrary shape in a porous medium', *Int. Commun. Heat Mass Transfer*, Vol. 11, pp.377–384.

Lu, W., Zhao, C.Y. and Tassou, S.A. (2006) 'Thermal analysis on metal-foam filled heat exchangers. Part I: Metal-foam filled pipes', *Int. J. Heat Mass Transfer*, Vol. 49, pp.2751–2761.

Ma, X.H. and Wang, B.X. (1998) 'Film condensation heat transfer on a vertical porous-layer coated plate', *Science in China (Series E)*, Vol. 41, pp.169–175.

Masoud, S., Al-Nimr, M.A. and Alkam, M. (2000) 'Transient film condensation on a vertical plate imbedded in porous medium', *Transport in Porous Media*, Vol. 40, pp.345–354.

Nusselt, W. (1916) 'Die Oberflachenkondensation des Wasserdampfes', *Zeitschrift des Vereines Deutscher Ingenieure*, Vol. 60, pp.541–569.

Patankar, S.V. (1980) *Numerical Heat Transfer and Fluid Flow*, McGraw-Hill, New York.

Popiel, C.O. and Boguslawski, L. (1978) 'Heat transfer by laminar condensation on sphere surfaces', *Int. J. Heat Mass Transfer*, Vol. 18, No. 1, pp.486–488.

Sukhatme, S.P., Jagadish, B.S. and Prabhakaran, P. (1990) 'Film condensation on single horizontal enhanced condenser tubes', *ASME J. Heat Transfer*, Vol. 112, pp.229–234.

Tao, W.Q. (2005) *Numerical Heat Transfer*, 2nd ed., Xi'an Jiaotong University Press, Xi'an.

Wang, S.C., Chen, C.K. and Yang, Y.T. (2005) 'Film condensation on a finite-size horizontal wavy plate bounded by a homogenous porous layer', *Appl. Thermal. Engrg.*, Vol. 25, pp.577–590.

Wang, S.C., Chen, C.K. and Yang, Y.T. (2006) 'Steady filmwise condensation with suction on a finite-size horizontal plate embedded in a porous medium based on Brinkman and Darcy models', *Int. J. Thermal Sci*., Vol. 45, pp.367–377.

Wang, S.C., Yang, Y.T. and Chen, C.K. (2003) 'Effect of uniform suction on laminar film-wise condensation on a finite-size horizontal flat surface in a porous medium', *Int. J. Heat Mass Transfer*, Vol. 46, pp.4003–4011.

Nomenclature

a	Thermal diffusivity $(\mathrm{m}^2 \cdot \mathrm{s}^{-1})$
c	Specific heat capacity $(\mathrm{J} \cdot \mathrm{kg}^{-1} \cdot \mathrm{K}^{-1})$)
d_f	Fibre diameter (m)
d_p	Pore diameter (m
g	Acceleration of gravity $(\mathrm{m} \cdot \mathrm{s}^{-2})$
h	Heat transfer coefficient $(\mathrm{W} \cdot \mathrm{m}^{-2} \cdot \mathrm{K}^{-1})$
Ja	Jacobi number
K	Permeability
k_e	Effective thermal conductivity $(\mathrm{W} \cdot \mathrm{m}^{-1} \cdot \mathrm{K}^{-1})$
k_l	Thermal conductivity of liquid $(\mathrm{W} \cdot \mathrm{m}^{-1} \cdot \mathrm{K}^{-1})$
q_m	Mass flow (kg/s)
Nu	Nusselt number
Re	Reynolds number
r	Latent heat of vapourisation $(\mathrm{J} \cdot \mathrm{kg}^{-1})$
T	Temperature (K)
u	Velocity $(\mathrm{m} \cdot \mathrm{s}^{-1})$
x	Position along x direction (m)
y	Position along y direction (m)
Greek symbols	
δ	Condensate thickness (m)
ε	Porosity
μ	Dynamic viscosity $(\mathrm{kg} \cdot \mathrm{m}^{-1} \cdot \mathrm{s}^{-1})$
ω	Pore density (PPI
ρ	Density $(\mathrm{kg} \cdot \mathrm{m}^{-3})$
Subscripts	
e	Effective
f	Fluid
1	Liquid
s	Saturation
v	Vapour
w	Wall